AN AERODYNAMIC COMPARISON OF BLOWN AND MECHANICAL HIGH LIFT AIRFOILS

John E. Carr
Grumman Aerospace Corporation

ABSTRACT

Short Takeoff and Landing (STOL) performance utilizing a circulation control airfoil was successfully demonstrated on the A-6/CCW in 1978 (Pugliese, 1979). Controlled flight at speeds as slow as 67 knots was demonstrated. Takeoff ground run and liftoff speed reductions in excess of 40 and 20% respectively were achieved. Landing ground roll and approach speeds were similarly reduced. This type of operational capability has been recognized as being advantageous in many future aircraft design studies (Hudson, 1981; Landfield, 1984). The A-6/CCW, however, was intended as a STOL demonstration vehicle only. It was limited by design to low speed flight. In 1981 the Navy accepted a proposal by Grumman Aerospace Corporation to develop and build a new generation of STOL demonstrator. The technology demonstrated was intended to be useable on modern high performance aircraft. STOL performance would be achieved through the combination of a 2-D vectored nozzle and a circulation control type of high lift system. The primary objective of this demonstration effort would be to attain A-6/CCW magnitude reductions in takeoff and landing flight speed and ground distance requirements using practical bleed flow rates from a modern turbofan engine for the blown flap system. Also, cruise performance could not be reduced by the wing high-lift system. The A-6 was again selected as the optimum demonstration vehicle. The goals and further discussion of the A-6 STOL demonstrator were presented by Carr (1984). This paper will document the procedure and findings of a study conducted to select the optimum high-lift wing design. Some findings of a separate study using a supercritical airfoil and a comparison of 2-D and 3-D results will also be described.

NOMENCLATURE

2-D	two dimensional, having an effective aspect ratio approaching infinity
3-D	three dimensional, having span, chord, and thickness
α_g	geometric angle-of-attack
C_ℓ	2-D lift coefficient
C_L	3-D lift coefficient, L/qS
C_d	2-D drag coefficient
C_m	2-D or 3-D pitching moment coefficient (subscript indicates reference location)
C_μ	blowing momentum coefficient, $\dot{m}V_j/qS$ ($\dot{m}V_j/qc$, if $\dot{m}$ is per unit span)
CCW	circulation control wing
c	chord length of original airfoil
c'	chord length with leading and trailing edges deployed
c_F	chord length of the flap
FT	abbreviation for foot
h	blowing slot gap height
GAP	height from flap or slat surface normal to wing surface
in	abbreviation for inch
R	radius of Coanda surface, expressed in percent chord (subscript 1 for dual radius indicates leading radius, 2 indicates aft radius)
t_{TE}	trailing edge thickness of cruise airfoil
q	tunnel dynamic pressure, expressed in pounds per square foot
R_n	Reynolds number
σ_F	trailing edge flap deflection, expressed in degrees
σ_S	leading edge slat deflection, expressed in degrees
σ_V	vane deflection on double slotted flap
C_{ℓ_α}	linear portion of lift curve slope, C_ℓ vs α
$C_{\ell_{max}}$	maximum lift coefficient
α_{stall}	angle of stall, deg
C_{d_o}	minimum drag level
V_{TRUE}	true airspeed, expressed in knots
S, S_{REF}	wing reference area in square feet
S_{BLOWN}	area of 3-D wing with blown trailing edge, ft^2
$\dot{m}$	mass flow through blowing slot in lb_f/sec^2, or $lb_f/ft/sec^2$
V_j	calculated isentropic jet exit velocity in ft/sec^2

INTRODUCTION

Pneumatic augmentation of the fluid surrounding an airfoil section to further amplify lift has received significant attention for several decades. The goal has been to achieve dramatic increases in lift over mechanically reconfigured wings, which changed their camber and/or area through the use of flaps and slats. The development of the jet flap and recognition of the Coanda effect have led to many innovative design concepts, several of which are illustrated in figure 1 along with applications of them. Two basic philosophies are involved. One is to obtain direct lift by exhausting a high momentum flow deflected to the flight path (ground attitude for hover and vertical flight). The jet flap accomplishes this by exhausting a deflected high momentum jet at the trailing edge of an airfoil (Deckert, 1985; Malavard, 1956). Lift is increased by the jet reaction and because the jet effectively extends the wing chord by maintaining a pressure differential above and below it, acting to increase effective wing area and moving the center of pressure rearward. Using the high momentum jet at the trailing edge of a flap, called a jet flap, has the added advantage of inducing increased circulation over the wing (Spence, 1956; Williams, 1962; Mashell, 1959; Schubauer, 1933). Both methods result in increased aerodynamic lift. Jet engine exhaust can also be deflected through rotating nozzles to obtain direct powered lift as on the Harrier (DeMeis, 1985). Deflecting the engine thrust at the wing trailing edge also results in deflected jet lift and increased circulation lift. This can be achieved by the placement of an engine nozzle either over or under the wing or through a properly designed nozzle placed adjacent to the wing trailing edge. This is not as efficient as the jet flap, but eliminates the need for large ducts in the wing and the much larger momentum of the engine has a much higher C_L potential.

Another approach to powered lift augmentation is the blown flap. Unlike the jet flap, the high momentum jet is placed in front of a mechanically deflected flap. This type of augmentation, called chordwise blowing, utilizes the Coanda effect to attach a thin, high momentum sheet of air (or other fluid) to the curved surface of a flap or cylinder. Initially, the sheet of air energizes the boundary layer and keeps the flow attached through large deflection angles due to a balance of centrifugal forces and the pressure differential. This increases wing circulation and entrains more of the freestream air, resulting in a significant increase in lift generated by the wing at low momentum levels. As the amount of blowing is increased, supercirculation of the flow around the airfoil causes the lift to increase

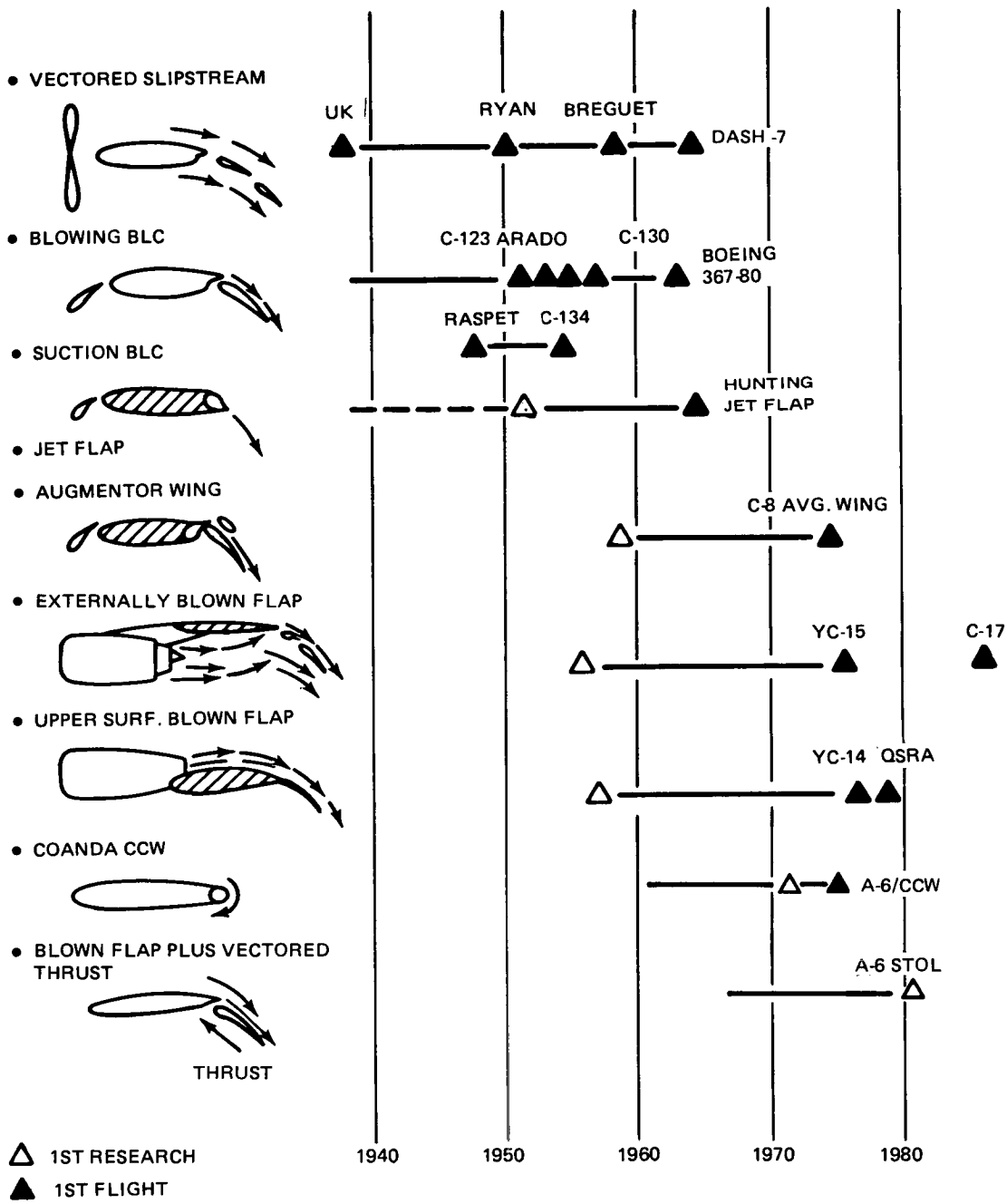

Figure 1. Powered lift chronology.

further. The maximum amount of increased lift is dependent upon the total turn angle of the curved surface and the available momentum. In the case of a 180-deg circular surface, as on the A-6/CCW, the flow can be made to wrap around the airfoil and return on the upper surface (Englar, 1975). The lack of a sharp trailing edge allows control of the stagnation point and greatly increases the circulation around the airfoil. Large increments in $\Delta C_\ell / C_\mu$ can be achieved at relatively low

C_μ values. Tangential and spanwise blowing can be used on leading or trailing edge devices to maintain attached flow and increase lift (Banks, 1984). Suction can also be used to remove the boundary layer to maintain laminar flow and delay separation. The F-4 and other designs have used leading and trailing edge blowing to provide improved takeoff and landing performance.

The NASA Quiet Short-haul Research Aircraft (QSRA), YC-15 and YC-14, used a combination of deflected thrust and the Coanda effect to increase lift. The YC-15, which led to the C-17 (Holt, 1984), uses an externally blown flap where flaps are deflected in the path of the engine exhaust plume. The wing flaps turn the engine thrust downward, resulting in a direct lift component. Slots in the flaps permit a controlled amount of flow to pass onto the upper surface where it acts similiar to a blown flap. The QSRA and YC-14 use upper surface blowing, where the high momentum engine exhaust is vented over the upper surface of the wing (Cochrane, 1981; Queen, 1981). This flow attaches itself to the wing upper surface and is turned by the Coanda effect when a flap is deflected at the wing trailing edge. Both systems have advantages and disadvantages, but are effective powered lift systems (Yen, 1982). While not as efficient as the chordwise blown flap aerodynamically, they have higher momentum levels and avoid the ducting problems of blown flaps. This technique is not easily applied to all aircraft types, however.

Circulation Control Wings (CCW) have been investigated extensively at David Taylor Naval Ship Research Development Center (DTNSRDC) for a number of years (Nichols, 1980; Englar, 1970). This work has been devoted to the idea of developing non-mechanical high-lift systems, which would eliminate conventional mechanical trailing edge devices and all the complexities associated with them. The conventional trailing edge flap is replaced with a fixed curved trailing edge, usually circular. These circulation airfoils rely entirely on the Coanda effect and supercirculation to increase lift above cruise airfoil levels. Lift augmentation ratios of CCWs are much higher than for blown flaps and continue to increase lift through moderate C_μ levels. DTNSRDC proved this concept on the successful A-6/CCW demonstrator aircraft (Englar, 1979a). The A-6/CCW was built and test flown by Grumman under contract with DTNSRDC. STOL performance reductions exceeding 20% in takeoff and approach speed and 40% in takeoff and landing ground distances were demonstrated (Pugliese, 1979). Slow flight was demonstrated down to a speed of 67 knots with a wing C_L of 3.60 at 29-deg angle-of-attack. At this condition the aircraft showed no indication of wing stall. The thick trailing edge and large duct size of the design presented a significant increase in cruise drag. The A-6/CCW was

designed to demonstrate low speed flight and STOL performance only and was not intended for direct application to high performance aircraft design. Improved overall performance has been the subject of subsequent studies with CCW airfoils at DTNSRDC (Englar, 1979b).

Following the completion of the successful A-6/CCW demonstrator program, work continued at Grumman Aerospace Corporation to improve and find applications for this technology. The development of the 2-D ADEN nozzle (Capone, 1979; Doonan, 1983) and the increased engine thrust of modern turbine engines led to the concept of the A-6 STOL demonstrator. The design would use 2-D nozzles deflected 60-deg and a pneumatically augmented wing flap to provide the high C_ℓ's necessary for STOL performance. Each system would provide approximately 50% of the required STOL lift. The wing blowing system would be limited to a practical bleed level, dictated by the capabilities of the engine and allowable thrust losses to meet acceleration requirements. The A-6 nozzle location, at the wing root trailing edge, provides the added benefit of thrust-induced lift on the wing. With a properly designed 2-D nozzle located in this position, the induced lift with deflected thrust would enhance the total lift of the design. The mid-fuselage location of the nozzle also helped to minimize trim requirements of the pitching moment which results from the deflected thrust. Much of the design work is covered by Carr (1984).

A 2-D airfoil wind tunnel test series was planned to evaluate different blown flap systems and arrive at the optimum configuration for the planned engine bleed flow rates. The A-6/CCW airfoil section was capable of turning the flow 180-deg statically, causing a tuft extending behind the blowing slot to wrap itself around the airfoil. However, with a surrounding freestream, the actual turning was less. This was particularly true at low C_μ. Since only a modest amount of bleed flow air was available, the Grumman blown lift designs concentrated on flaps with less total turning arc, but a healthy initial blowing radius. The 2-D test was conducted at DTNSRDC concurrently with a separate DTNSRDC study to define advanced CCW sections. Both of these tests and a test of the A-6 high-lift system were conducted between November 1982 and February 1983. This paper provides the results of the 2-D test series and the evaluation process to select the A-6 STOL high-lift wing configuration. A comparison with results from a separate test on a 13% supercritical airfoil section and with tailoff 3-D wind tunnel data are also provided.

MODEL GEOMETRY

The trailing edge candidates compared in this paper and the 64A008.5 Mod airfoil are shown in figure 2 with some geometric comparisons presented in figure 3. The 64A008.5 Mod airfoil is shown with a 25-deg leading edge slat deflection and a 30% chord semi-Fowler single slotted flap deflected 30-deg. A 30% chord double-slotted Fowler flap was also tested and is presented for comparison with the blown flaps. A 17% chord vane deflected 20-deg and 24% chord flap deflected 40-deg showed maximum high-lift and minimum high-lift drag and was selected for comparison here. This flap retained the original A-6 airfoil shape when retracted. The plain blown flap, which has a large 6% chord leading edge radius blended smoothly into the original airfoil upper surface contour, is shown with 50-deg deflection. This was the maximum deflection possible without modifying the A-6 clean airfoil contour. The primary Grumman candidate, the 13% chord crescent blown flap, consisted of a continuous 8% chord radius upper surface extending from flap leading to trailing edges. A lower surface cusp at the trailing edge permitted a greater total arc and acts to turn the lower surface flow downward. A 6.5% chord crescent flap was also built. However, it was dropped from the test when the larger chord crescent flap failed to produce the expected lift and revealed that much of the achieved lift was due to the flap chord camber. Unlike the single slotted and plain blown flaps which have respectable thin airfoil trailing edges when retracted, the crescent blown flap retains its upper surface contour and has an equivalent trailing edge thickness of 2.8% of the chord. The airfoil also requires thickening beyond the 70% chord to accommodate this section with a maximum deflection of 43-deg. A flat trailing edge was also tested on the crescent flap. This was intended to reduce the retracted trailing edge thickness and provide a tradeoff between maximum high-lift and acceptable cruise drag. Unfortunately, the high-lift results were not impressive, although the clean airfoil drag was reduced. The model design may have affected the results since the flat trailing edge should have done as well as the full arc at low blowing coefficients.

A CCW section proposed by DTNSRDC with a 3.5%c' dual radius flap is also presented here. An analysis of the DTNSRDC CCW sections is contained in Englar's paper (1983). The dual radius configuration extends below the airfoil lower surface when deflected 90-deg by 0.035c'. The blowing surface is provided by two circular surfaces, joined tangentially to form a smooth upper surface curve to the trailing edge. This provides a sharp initial radius for maximum flow acceleration behind the nozzle and a gentler secondary radius to prevent separation and permit a total turn angle of 123-deg from the nozzle centerline. The leading circular surface has a 1.2% chord

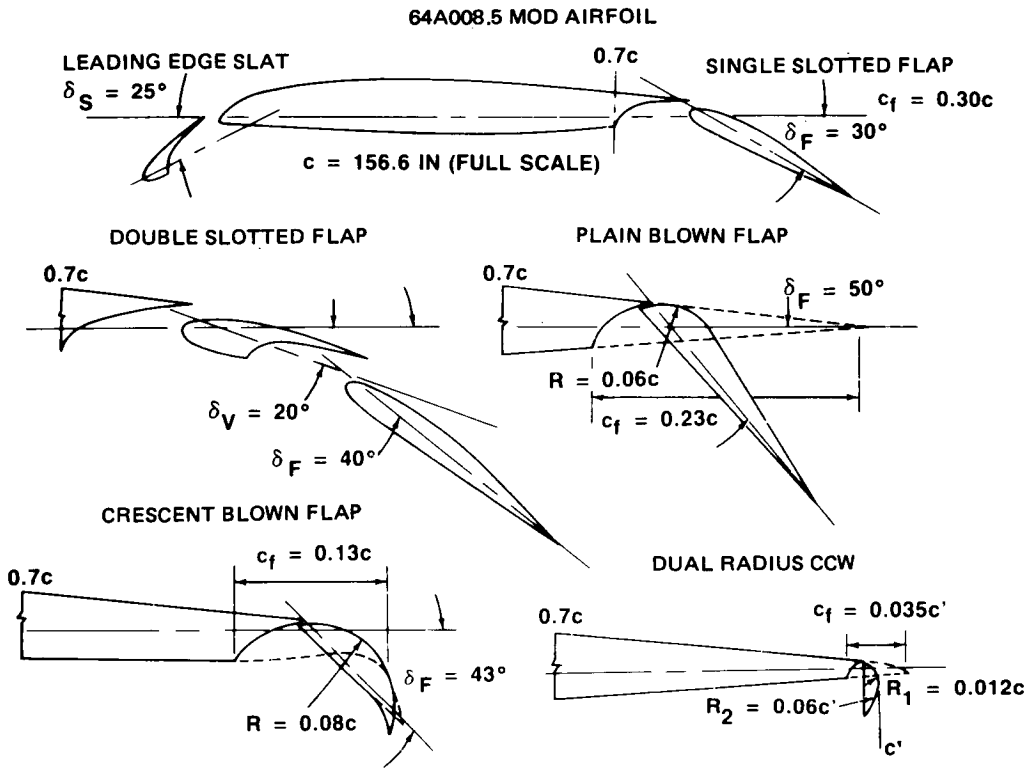

Figure 2. 2-D airfoil sections.

FLAP TYPE	C_f/C	R/C	t_{TE}/C	FLAP ANGLE ~ DEGREES	TOTAL TURNING ARC ~ DEGREES
SINGLE SLOTTED	0.30	—	0.0014	30	—
DOUBLE SLOTTED	0.30 (0.17/0.24)	—	0.0014	30 (20/40)	—
PLAIN BLOWN FLAP	0.23	0.06	0.0014	50	58
CRESCENT BLOWN FLAP	0.13	0.08	0.028	43	110
DUAL RADIUS CCW	0.035	0.012/0.06	0.0014	90	123
A-6/CCW	0.0730	0.0365	0.0730	180	180

Figure 3. Comparison of flap geometries.

radius while the aft surface has a much larger 6% chord radius. This flap is deployed 90-deg for maximum lift, with lesser deflections possible for maneuver and takeoff. Similar to the crescent flap, the dual radius CCW retains its upper surface curvature when retracted to zero deg, although the effective trailing edge thickness is the same as the A-6 airfoil. The impact of the resulting trailing edge camber on cruise lift and drag will be shown later. The A-6/CCW geometry is provided to demonstrate the dramatic reduction in size between it and the dual radius

CCW. The A-6/CCW had a 3.65% chord semi-cylindrical trailing edge with a 180-deg deflection. The effective trailing edge thickness in cruise was 7.3% of the chord.

TEST APPARATUS AND TECHNIQUE

The 2-D test was conducted in the DTNSRDC 8 X 10 ft subsonic wind tunnel between 3 X 8 ft 2-D double wall inserts. A 2-ft chord by 3-ft span 64A008.5 Mod section was installed on rotatable end plates flush to the wall inserts to obtain a 2-D condition. Pressures were recorded on a 144-port scani-valve system through pressure taps located chordwise at the mid-span location. Pressures were also recorded at the 1/4-span locations to check the 2-D spanwise distribution. The mid-span pressures were integrated over the chord to determine 2-D lift and pitching moment. A characteristic pressure distribution for the plain blown flap is shown in figure 4. Drag was measured by use of a drag rake located behind the mid-span station. A comparison of clean airfoil wake profiles is shown in figure 5. The rake pressure taps were spaced closely together to record the detailed variation in the wake pressure. Use of the drag rake resulted in questionable results for the high-lift airfoils, as will be discussed later. Tunnel test conditions were varied between a q of 10 psf for a Reynolds number of 1.2×10^6/ft to a q of 65 psf for a Reynolds number of 2.6×10^6/ft. The low q condition was used to obtain a greater range of C_μ. Most testing was conducted around a q of 35 psf to allow a reasonable C_μ range and Reynolds number compromise. C_μ was calculated by the product of the mass flow into the model per unit span, as measured by a venturimeter in the supply system and the calculated jet velocity using isentropic expansion based on the plenum pressure and static free stream pressure non-dimensionalised by the tunnel q and the deflected wing chord. Blowing momentum was provided through a plenum chamber in the model cavity and exhausted tangentially onto the flap upper surface through a spanwise slot located at the main airfoil section trailing edge. Plenum pressure was varied up to 60 psf. The test apparatus and test technique are described further by Englar (1979b, 1972a, and 1972b).

A leading edge dowel was used on the sharp lower leading edge of the main airfoil, which was exposed with the leading edge slat deflected, to prevent early separation at high-lift conditions. This also helped to improve the Reynolds number characteristics of the leading edge slat. Tests were conducted separately with this dowel in place and removed; without the dowel the leading edge separation was observed to occur early at low tunnel q's, showing a dramatic loss in lift at low

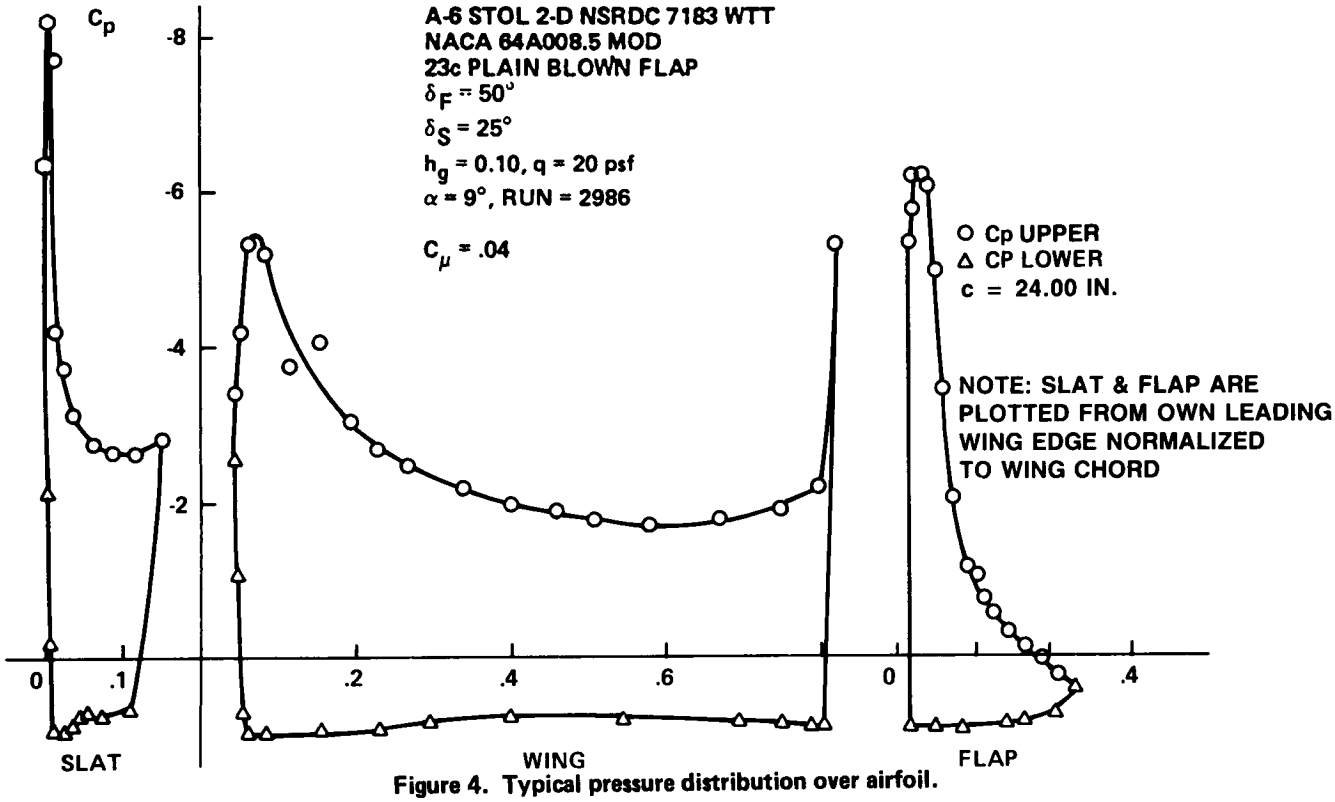

Figure 4. Typical pressure distribution over airfoil.

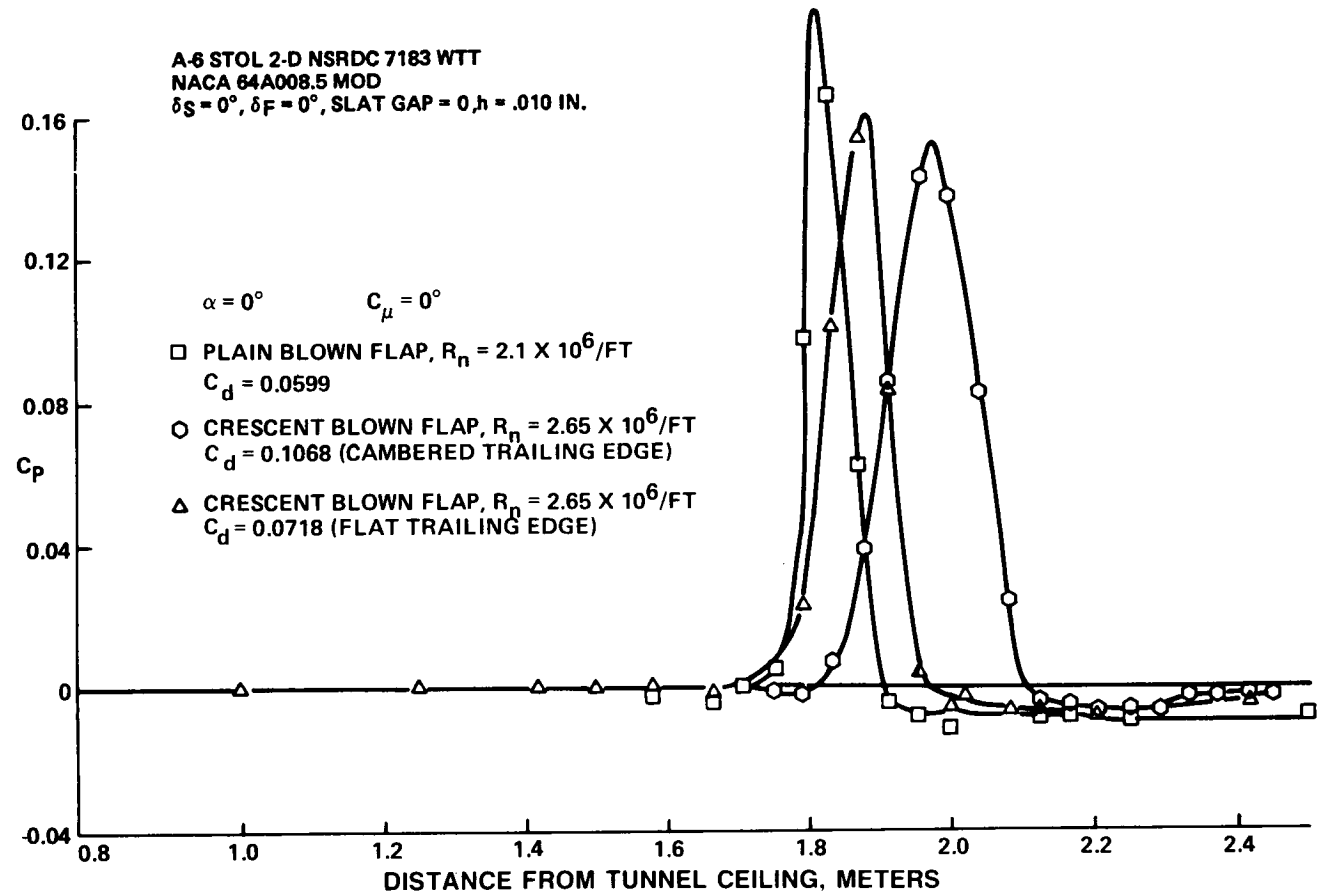

Figure 5. Wake rake drag measurement.

Reynolds numbers. Lift characteristics with the dowel appeared less dependent on Reynolds number. At higher tunnel q, representing a Reynolds number of 2.5×10^6, no difference was found in C_{ℓ_α} or $C_{\ell_{max}}$ with or without the dowel. The dowel was removed for the cruise configuration.

BLOWN FLAP BLC COMPARISON

A comparison of the 2-D blown flap C_ℓ's with blowing momentum coefficient C_μ is shown in figure 6. The data are presented for alpha geometric of 6-deg to avoid apparent stall regions at lower and higher angles-of-attack. The A64A008.5 Mod airfoil lifts with no flap or slat deflection, with the 30% chord semi-Fowler flap deflected 30-deg, and with the double slotted flap, are also shown on the left axis for comparison. Note that the highest lift for low blowing coefficients, C_μ less than 0.04, is obtained by the plain blown flap. This is due largely to the lift generated by the larger 23% chord flap at $C_\mu = 0$. Above $C_\mu = 0.04$ the dual radius achieves greater lift due to its greater turning arc. However, the lift is not significantly greater than the plain blown flap until $C_\mu = 0.08$. The crescent blown flap has nearly the same blowing-off lift as the plain blown flap, but requires substantial C_μ before the total C_ℓ becomes greater than that of the plain blown flap. This is due to the larger turning radius and larger total turning arc of the crescent flap. The data suggest that at even higher C_μ the crescent flap may do as well as the dual radius CCW.

All of the blown flaps produced more lift than the single slotted flap with very little blowing, C_μ less than 0.02. The double slotted flap C_ℓ is higher than the plain blown flap at C_μ below 0.02 and higher than the dual radius CCW at C_μ below 0.03. This indicates that for very low blowing rates, conventional flap design may be equivalent or better than blown flap systems, especially when weight, drag, and thrust loss tradeoffs are considered. To be effective for high performance aircraft, the augmented high-lift system must provide a significant increase in lift relative to the additional weight and complexity of incorporating it instead of a simple mechanical flap. It must also allow reasonable cruise drag levels and minimal thrust drain from the engine to meet acceleration requirements.

Greater total lift is produced by the plain blown flap at C_μ below 0.04 and by the dual radius above 0.04. The dual radius flap always produces a greater lift increment due to blowing, ΔC_ℓ vs. C_μ, as shown in figure 7. The plain blown flap produces equivalent BLC lift up to $C_\mu = 0.01$, but for higher C_μ the

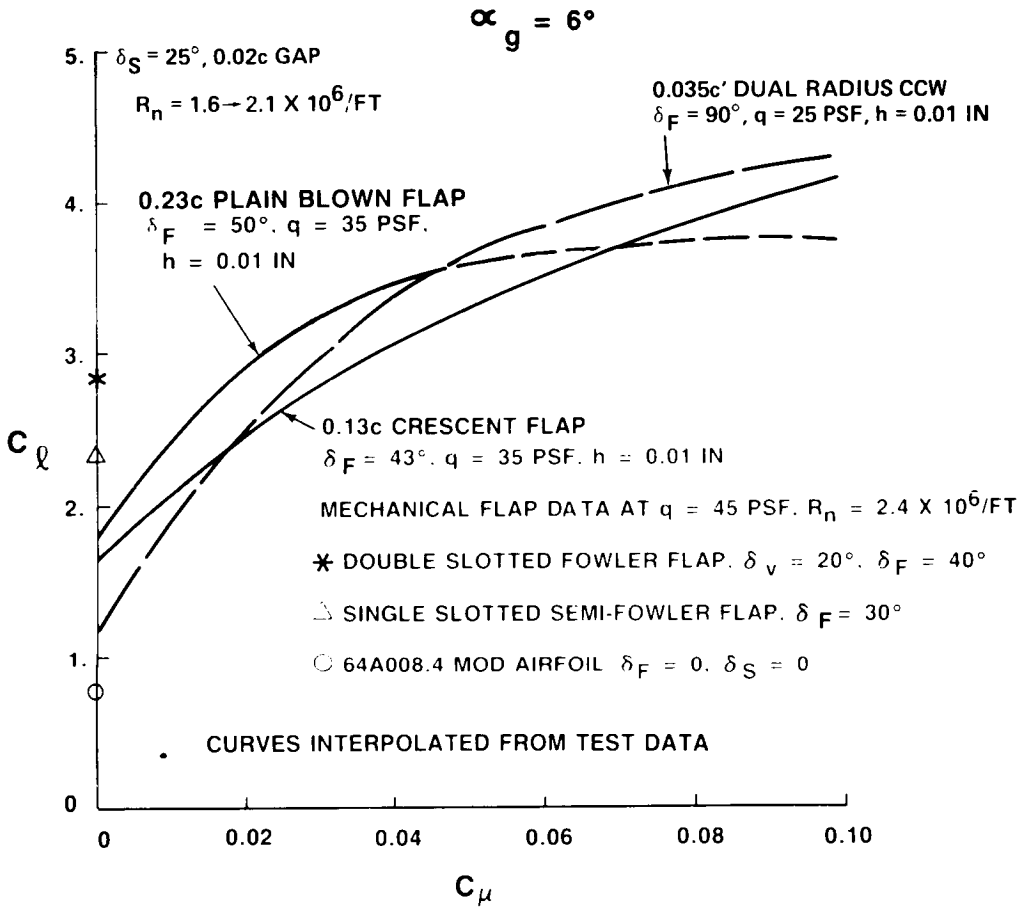

Figure 6. 2-D lift comparison, BLC-on.

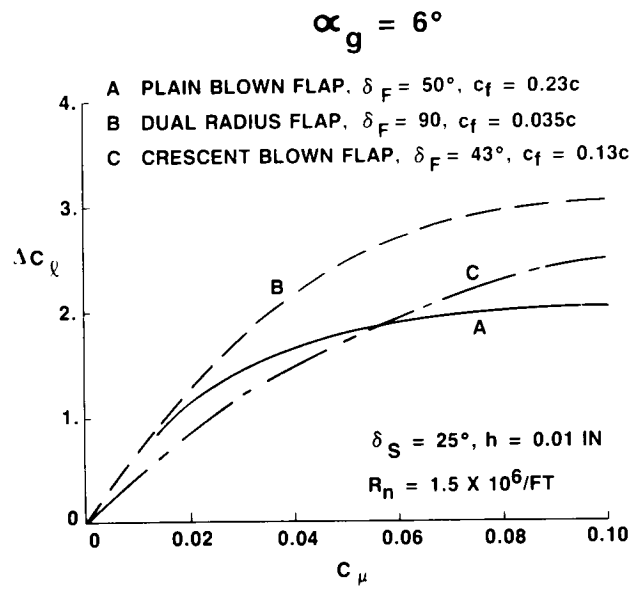

Figure 7. Lift increment due to blowing.

C_ℓ increase tapers off because of the limited turning arc. The plain blown flap shows a flattening in the C_ℓ versus C_μ curve above C_μ = 0.06. This is a familiar characteristic of blown flaps. Figure 8 shows that at alpha geometric = 0 deg, the dual radius CCW achieves an increment in C_ℓ nearly matching Glauert's potential flow theory up to C_μ of 0.02. At higher C_μ the C_ℓ is better than that reported by Lachmann for a 13% thick symmetrical airfoil with a 67.5-deg flap deflection (Lachman, 1961). The plain blown flap does as well as the 3.65% chord CCW at very low C_μ and slightly better at C_μ between 0.02 and 0.04. All of these flaps do significantly better than jet flap theory.

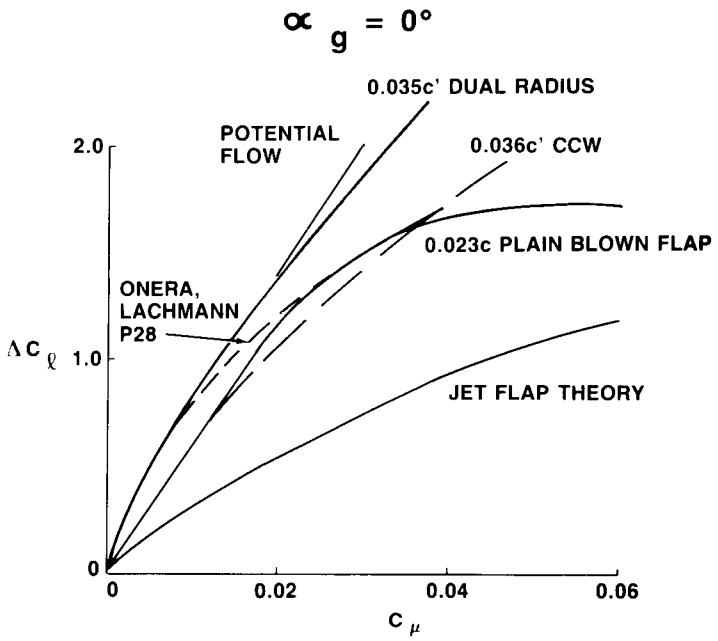

Figure 8. Lift increment comparison.

HIGH-LIFT SYSTEM EVALUATION

The benefits of the blown flap for a given design have been shown to relate directly to the blowing momentum, C_μ. Thus to evaluate the system properly, the aerodynamic characteristics must be compared at the intended operational C_μ, which is limited by the momentum available to the design. Figure 9 shows the A-6/STOL full-scale C_μ variation with velocity based on the amount of bleed air momentum, $\dot{m}V_j$, available from the A-6 STOL powerplants. For designs with large amounts of blowing momentum available to them it may be possible to optimize C_μ to provide maximum performance, as was done on the A-6/CCW. However, where limited amounts of bleed air are available, the available momentum may impose a design C_μ. The 2-D

equivalent C_μ is calculated by multiplying the 3-D C_μ by the ratio of the 3-D blown flap area to reference wing area. Thus at a predicted approach speed of between 82 and 92 knots, the 2-D equivalent C_μ is approximately 0.04. The predicted approach speed is based on estimated aero data and discussions with NAVAIR concerning useable STOL performance improvements. The aerodynamic data was estimated from A-6/CCW flight test results adjusted for configuration differences of this design. Navy personnel indicated that approach speeds below 80 knots would cause pattern congestion when mixed with current carrier aircraft whose typical approach speeds are well in excess of 100 knots. Also, the A-6/CCW demonstrated that aircraft handling characteristics were severely degraded at speeds below 80 knots.

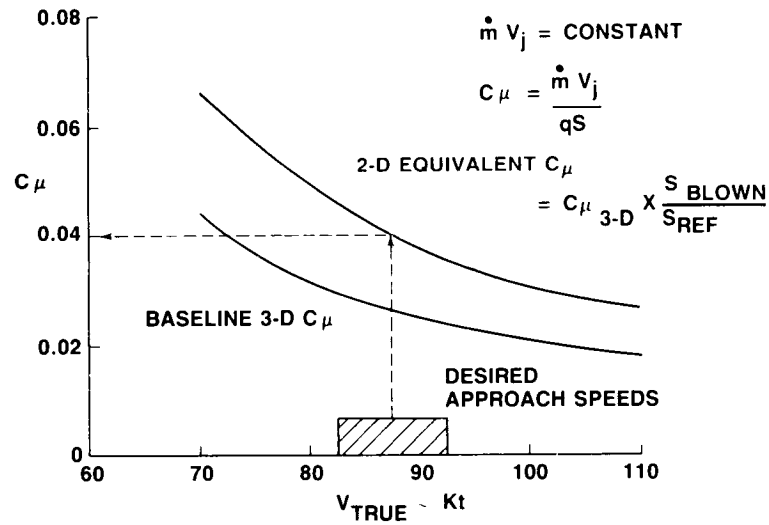

Figure 9. 2-D equivalent C_μ.

A comparison of C_ℓ vs α for C_μ = 0.04 (fig. 10), shows the lift of the plain blown flap and dual radius CCW is nearly equivalent at low alpha. However, the dual radius flap stalls out at alpha of 9-deg and a $C_{\ell_{max}}$ of 3.35; C_{ℓ_α} is also slightly reduced. The plain blown flap stalls at α = 10 deg with a $C_{\ell_{max}}$ of 3.55, increasing the clean airfoil lift three and one-half times. While this is a much lower augmentation ratio than can be achieved by a pure CCW, it is sufficient to meet the desired performance gains. Full scale Reynolds number effects may also increase α stall. The dual radius $C_{\ell_{max}}$ could be increased by some leading edge treatment; however, the stall would have to be delayed to 13-deg α to achieve the same $C_{\ell_{max}}$ as the blown flap. The lift of the single slotted flap is increased by a third with the plain blown flap at C_μ = 0.04. The reduction in α stall indicates that some leading edge treatment would be useful. However, wing mechanical limitations and cruise

performance must also be considered. The crescent blown flap C_ℓ is nearly equivalent to the double slotted flap at this condition, with the crescent flap exhibiting a higher C_{ℓ_α} and a lower α stall, but nearly the same $C_{\ell_{max}}$. Comparing $C_{\ell_{max}}$ at $C_\mu = 0.04$ for the blown high-lift systems, the plain blown flap has the highest $C_{\ell_{max}}$, with the dual radius and crescent blown flap being nearly equal to the double slotted flap.

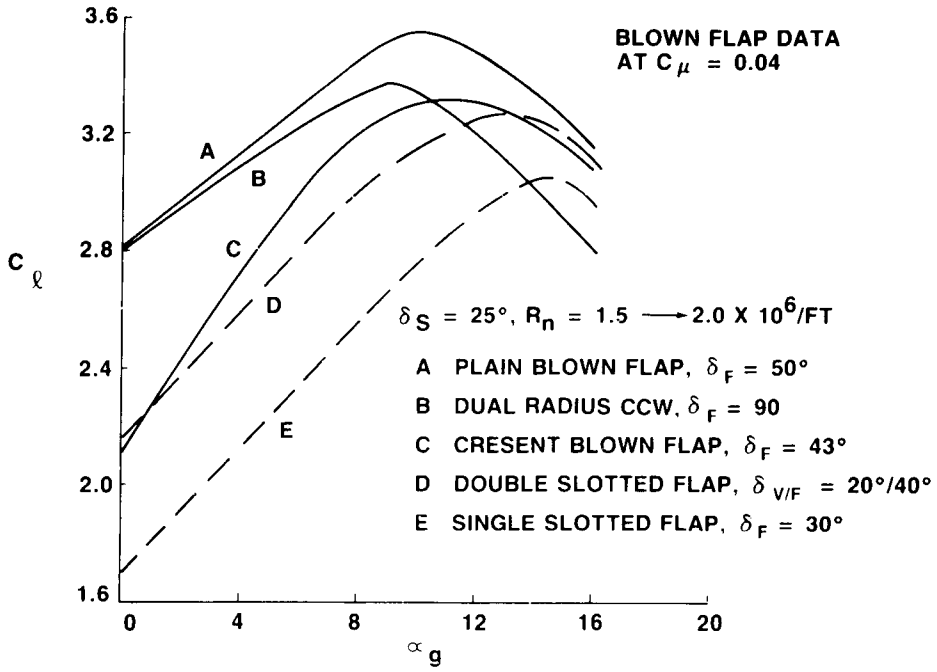

Figure 10. 2-D lift comparison at approach conditions.

The plain blown flap and crescent flap $C_{\ell_{max}}$ are nearly equal at $C_\mu = 0$. The double slotted flap $C_{\ell_{max}}$ is higher than any of the blown flaps, and the lift is nearly triple that of the clean airfoil. At the lower C_ℓ of the blown flaps at $C_\mu = 0$, the flow remains attached on the leading edge slat through higher angles and results in a higher alpha stall than the single or double slotted flaps. The tradeoff between the larger chord plus larger deflection of the plain blown flap, and the upper surface curvature of the crescent flap becomes obvious as both produce about two thirds the lift of the double slotted flap at low alphas. The very small chord dual radius, on the other hand, has half the lift increment of the crescent or plain blown flaps. This impressive result with almost one seventh the chord is due to its curved upper surface and the high flap deflection angle. The baseline airfoil C_ℓ versus alpha is shown for comparison along with the increase in α_{stall} obtained with slat deflection.

Blowing-off lift was important to the demonstrator program (fig. 11). Safety considerations for the demonstrator and for future applications, in case of loss of the blowing system, required a reasonable approach C_ℓ without blowing. Too low a C_ℓ at $C_\mu = 0$ could result in an approach speed that would endanger the aircraft. A part of the test program would be to measure STOL gains using vectored thrust alone and in combination with the blown flap system. Thus, good $C_\mu = 0$ lift is a basic requirement of the design. The C_ℓ level of the plain blown flap at $C_\mu = 0$ and a deflection of 50-deg for approach was deemed acceptable for the demonstrator.

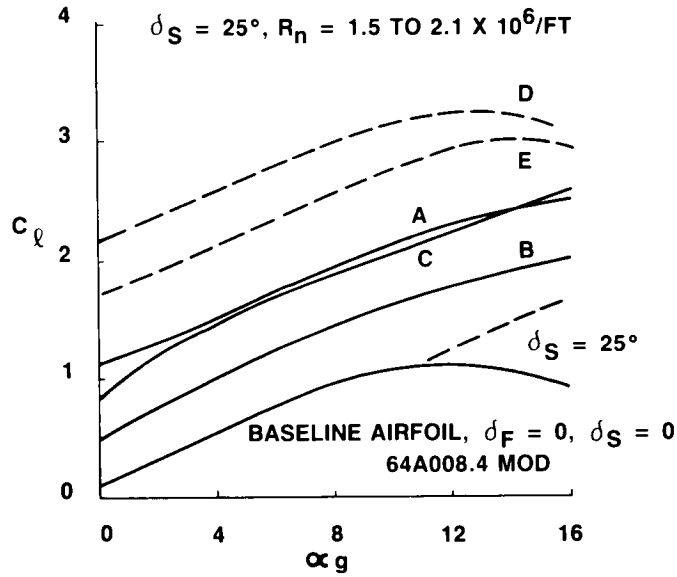

Figure 11. 2-D lift comparison at $C_\mu = 0$.

Another concern in selecting the optimum high-lift system is the amount of pitching moment required to trim. Figure 12 provides a comparison of the 2-D C_m at approach conditions. All of the blown flaps have a more negative C_m than the mechanical flaps due to the amount of lift concentrated at the flap leading edge with very high pressure peaks. The dual radius flap shows over twice the nose-down moment of the mechanical flaps due to the blowing slot and flap pressure peak located at the wing trailing edge, furthest aft of the aerodynamic reference. The increase in C_m also indicates trim lift and downwash would be larger for the blown flaps, resulting in less total lift for some aircraft configurations. The pitching moment for the dual radius is approximately equal to the A-6/CCW moment, which required extensive modification of the horizontal tail to trim. The plain blown flap may also require some horizontal tail redesign for an A-6 configuration, but it would be less extensive than that for the dual radius.

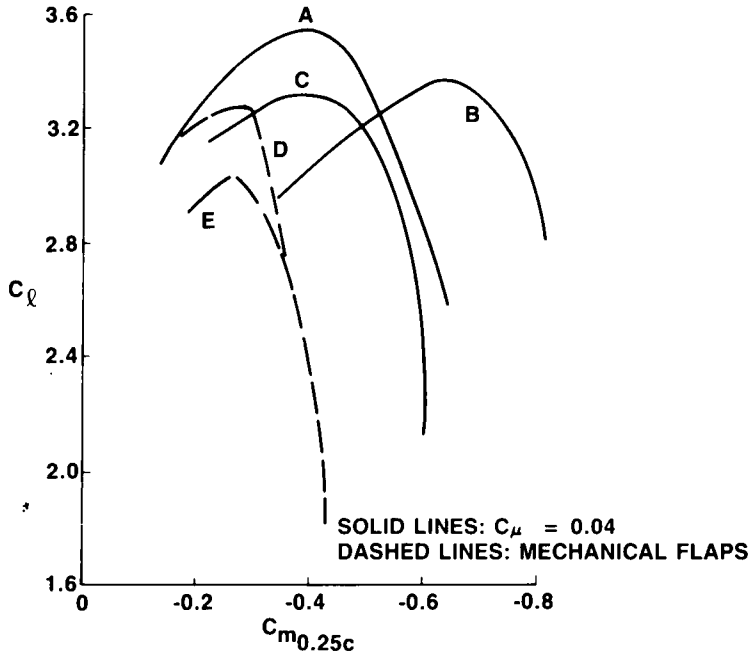

Figure 12. Comparison of C_m.

The clean airfoil drag for the plain, dual radius, and crescent blown flaps is shown in figure 13. To meet the cruise design requirement, the clean airfoil drag must not be increased by the flap system. The retracted plain blown flap which has the same contour as the original airfoil meets this requirement, as do the single and double slotted flaps. The dual radius and crescent blown flap both increase C_{d_o}. The dual radius CCW produces a lower C_d than the original airfoil above $C_\ell = 0.4$, which may improve some point performance. The dual radius C_ℓ for C_{d_o} is higher than for the original airfoil, indicating an increase in C_ℓ at alpha = 0 as well in the retracted position. The crescent flap C_{d_o} represents an unacceptable penalty on the design. Oil flow studies indicated separation on the crescent flap at 72% of the flap chord in the retracted position. Blowing over the retracted crescent flap did result in decreased drag with increased lift. However, stall occurred at a much lower alpha and the thrust drain from the engine would increase engine fuel flow which may not be acceptable. Higher Reynolds number conditions will also move the separation further aft and decrease separation drag somewhat. A flat trailing edge section tested on the crescent flap showed a drag increase about half that of the full crescent flap. C_ℓ vs α and C_μ characteristics for this section were unimpressive, however.

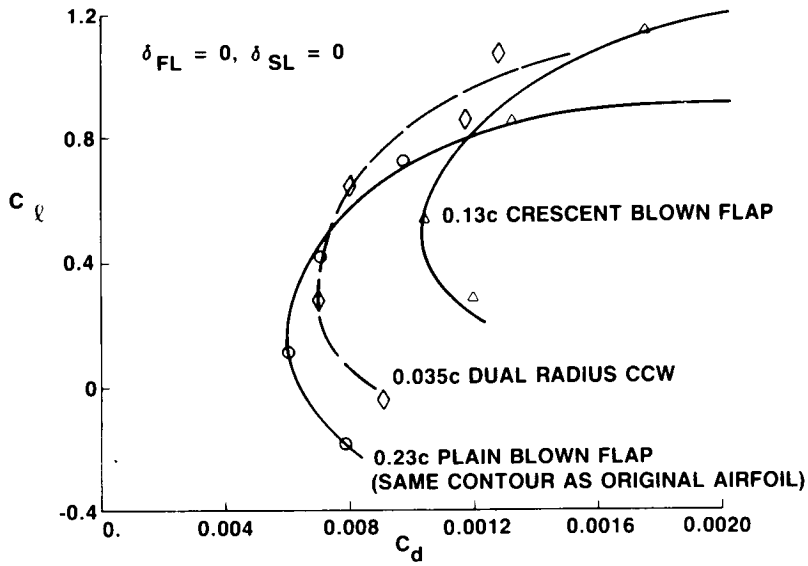

Figure 13. 2-D clean airfoil drag.

A comparison of high-lift system drag would be useful. However, the use of a drag rake to measure blowing-on drag had a questionable result in the view of some Grumman engineers. Figure 14 shows C_d decreases dramatically with increasing C_μ. The dashed $C_d - (-C_\mu)$ line shows that the decrease is much greater than the full value of the forward thrust of the jet at the nozzle exit. This is an optimistic approach that ignores the jet deflection component and flow mixing losses. Typical wake rake pressure profiles that were integrated to obtain the C_d vs C_μ curve on the left are shown on the right. With blowing-off, a nice pressure distribution exists. As blowing is increased, the pressure variation becomes smaller ($C_\mu = 0.02$) until it actually reverses ($C_\mu = 0.04$) and becomes a thrust. The height of the pressure peak relative to the airfoil also increases. Some 2-D drag reduction is expected due to the decreased separation. However, some of the data indicate $C_d + C_\mu$ values less than zero, suggesting negative profile drag. Pope (1966) states, "The wake survey cannot be used to measure drag of the stalled airfoils or of airfoils with flaps down. Under these conditions a large part of drag is caused by rotational losses and does not appear as a drop in linear momentum." Futher study of methods to measure drag with highly rotational flows may be indicated.

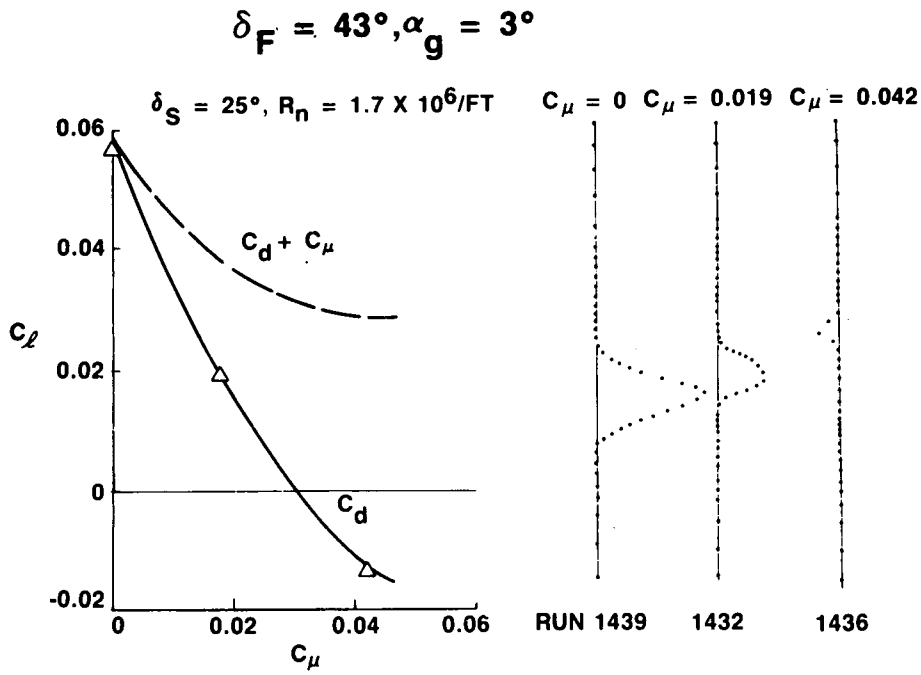

Figure 14. Determination of drag with BLC - on crescent blown flap.

PLAIN BLOWN FLAP RESULTS

This evaluation of lift, drag, and pitching moment for these high-lift systems, in both high-lift and cruise configurations, shows obvious advantages with the plain blown flap for the A-6 STOL demonstrator. The plain blown flap provides higher C_ℓ in the desired C_μ range, has a higher $C_{\ell_{max}}$, higher C_ℓ at $C_\mu = 0$ than the dual radius (its closest competitor), lower trim moment than the dual radius, and a lower C_{d_o} than the other blown flaps. Other test results show that C_ℓ will be even larger with full scale Reynolds number and with increased slot height.

The lift and pitching moments of the plain blown flap are shown in figure 15 as functions of α and C_μ. The increase in lift due to C_μ flattens out above $C_\mu = 0.06$. There is some reduction in α for $C_{\ell_{max}}$ with C_μ suggesting possible leading edge improvements could be made. The C_m curve shows an acceptable nose-down increase in pitching moment with the addition of blowing. Too large an increase in C_m with C_μ could indicate poor transition characteristics that would provide an increased workload for the pilot.

The tests indicated other interesting results as well. All of the data shown earlier used a blowing slot height of 0.01-in. When the slot height was doubled to 0.02-in for the plain blown flap deflected 43-deg (fig. 16), a fair increase in lift resulted. The lift of the plain blown flap with δ_F = 43-deg was increased as much

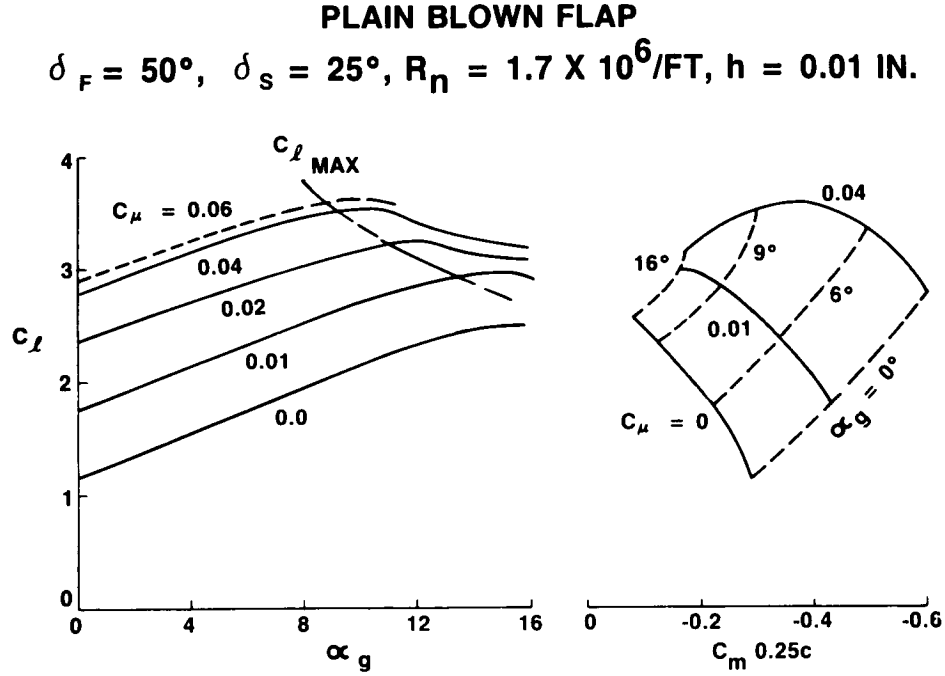

Figure 15. Variation in C_ℓ & C_m with C_μ & α_g.

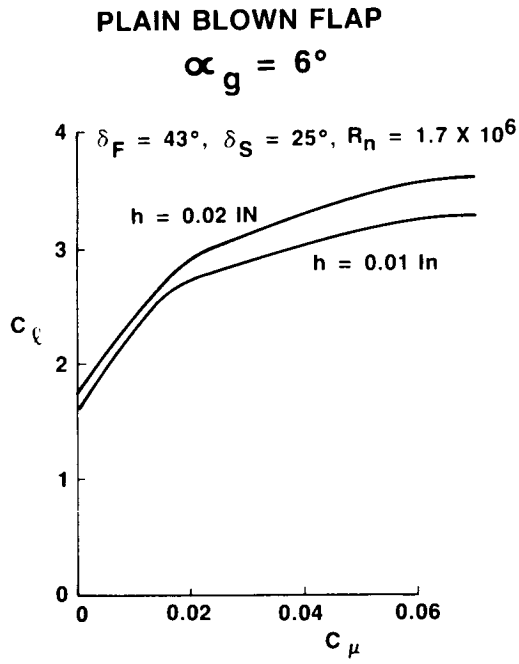

Figure 16. Effect of slot gap height on lift.

by doubling the slot height to 0.02-in as increasing the flap deflection from 43-deg to 50-deg (not shown). These results indicate that even larger lift increments than those shown in the previous curves are possible with increased slot height. The opposite effect was found by increasing slot height on the crescent flap.

The tests were conducted at a q of 35 psf for a Reynolds number of 1.6 x 10^6/ft to obtain data over a reasonable C_μ range. The effect of Reynolds number on the data was checked by increasing tunnel q to 45 psf and 65 psf for Reynolds numbers of 2.1 and 2.6 x 10^6/ft respectively. A significant increase in C_ℓ results with increasing Reynolds number at all C_μ levels (fig. 17).

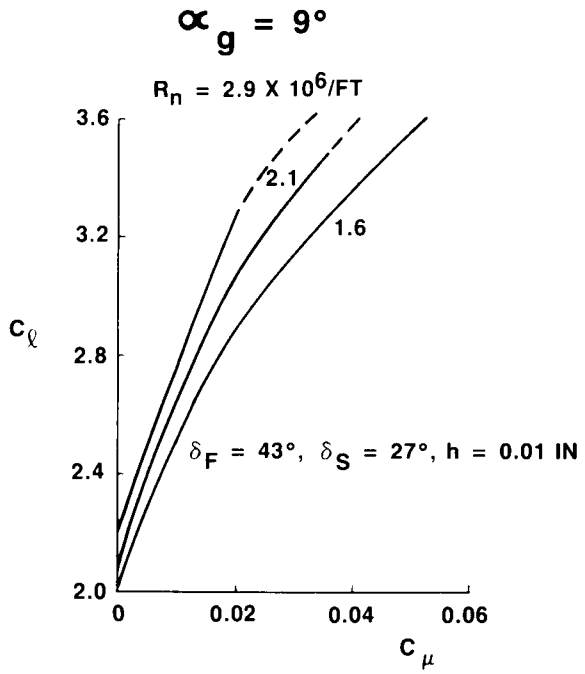

Figure 17. Effect of Reynolds number on C_ℓ.

SUPERCRITICAL SECTION COMPARISON

A separate test was conducted in the Grumman low-speed wind tunnel of a 13% thick airfoil with similar trailing edge high-lift devices. The airfoil and four high-lift devices are shown in figure 18. They are a 30% chord single slotted flap deflected 30-deg, a 30% chord double slotted flap with a 40-deg vane deflection and 50-deg flap deflection, a 23% chord plain blown flap, and a 13% chord crescent blown flap both with deflections of 43-deg.

The plain blown and crescent blown flaps were expected to have better cruise drag and high lift performance with this airfoil since they blend in well with the original airfoil lines. Also, the airfoil has some upper surface trailing edge curvature, which could help the plain blown flap by providing a secondary turning radius with a larger turning angle than the 64 series aft section did.

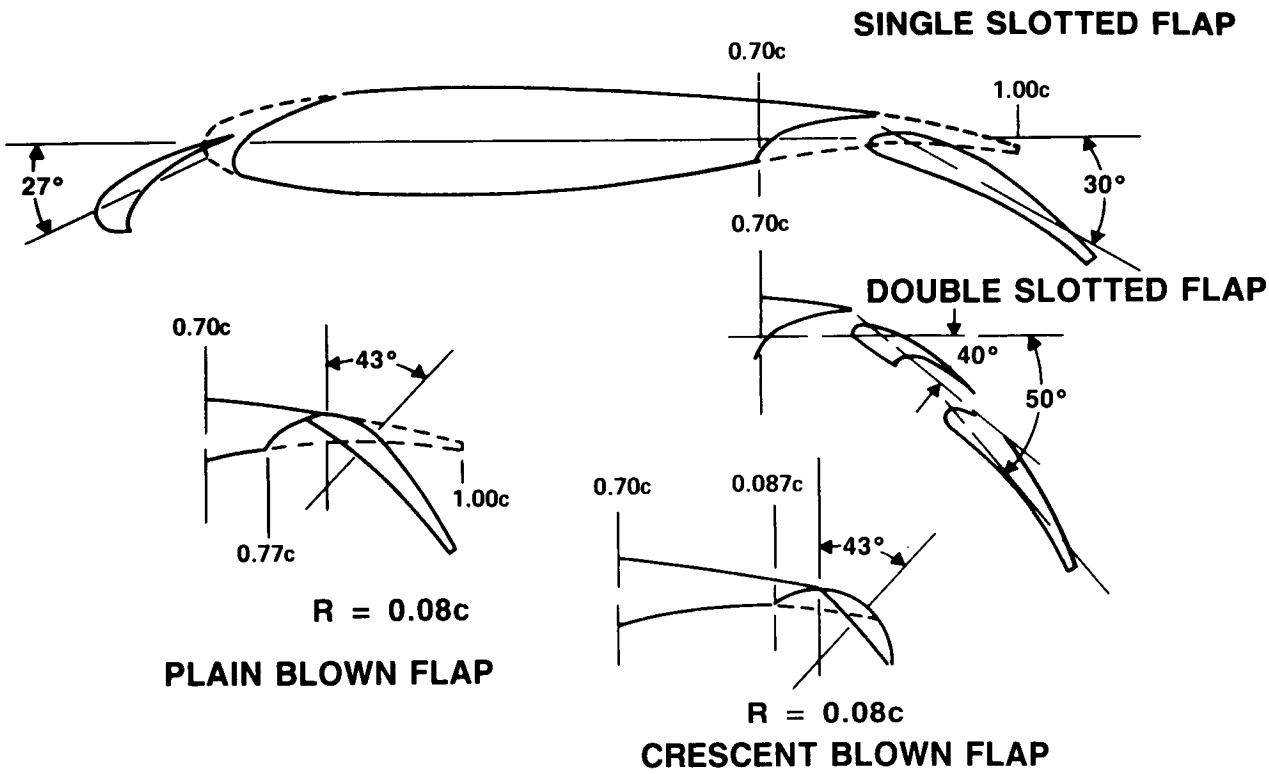

Figure 18. 0.13c supercritical sections.

C_ℓ is shown in figure 19 versus C_μ for alpha = 10-deg and δ_s = 27-deg. The direct lift comparison shown indicates much better performance for the crescent blown flap than was seen for the 64A series airfoil. The double slotted flap also performs quite well, yielding as much lift as the crescent flap up to C_μ = 0.04 and the plain blown flap up to C_μ = 0.055. The characteristic flattening of C_ℓ with increasing C_μ is less evident for the plain blown flap than for the 64A series airfoil. The contour of the supercritical trailing edge apparently works as a secondary radius.

The increase in $C_{\ell_{max}}$ with leading edge slat deflection (fig. 20) is dramatic for the plain blown flap. $C_{\ell_{max}}$ increases by more than ΔC_ℓ = 1.0 with a 27-deg leading edge slot deflection for the whole C_μ range.

Blowing slot height was also investigated. Figure 21 indicates C_ℓ is sensitive to blowing slot height and that an optimum slot height can be found for a given configuration. Here the 0.014-in height always produces the greatest lift. The narrow 0.006-in height becomes more effective as C_μ increases. This may, however, be the result of the slot height increasing under increased plenum pressure as C_μ is increased.

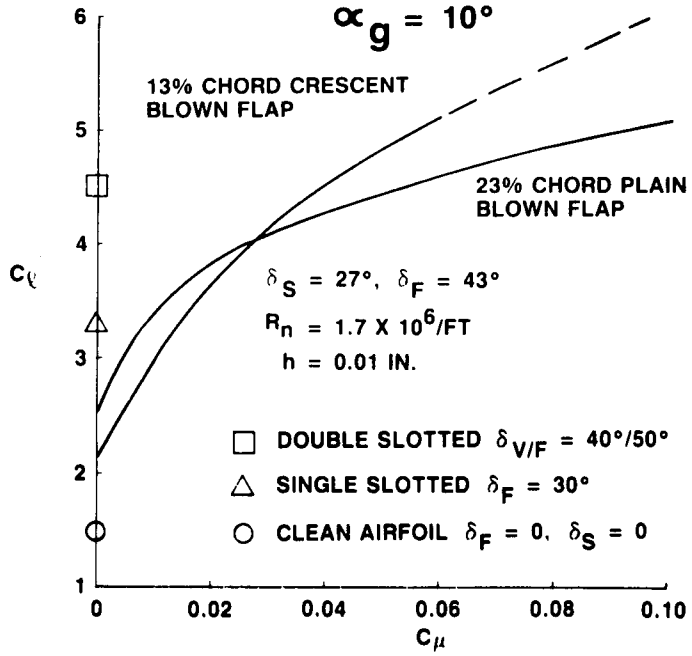

Figure 19. Comparison of C_ℓ for a 13% supercritical airfoil.

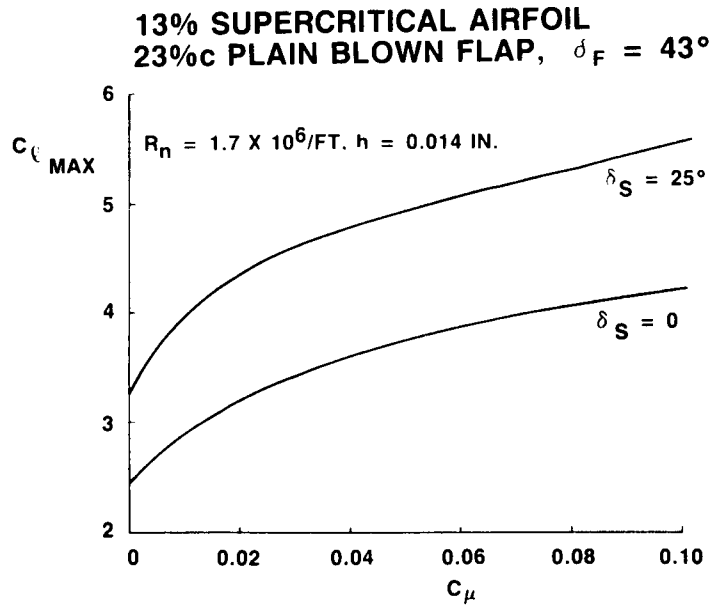

Figure 20. Effect of slat deflection on $C_{\ell_{MAX}}$.

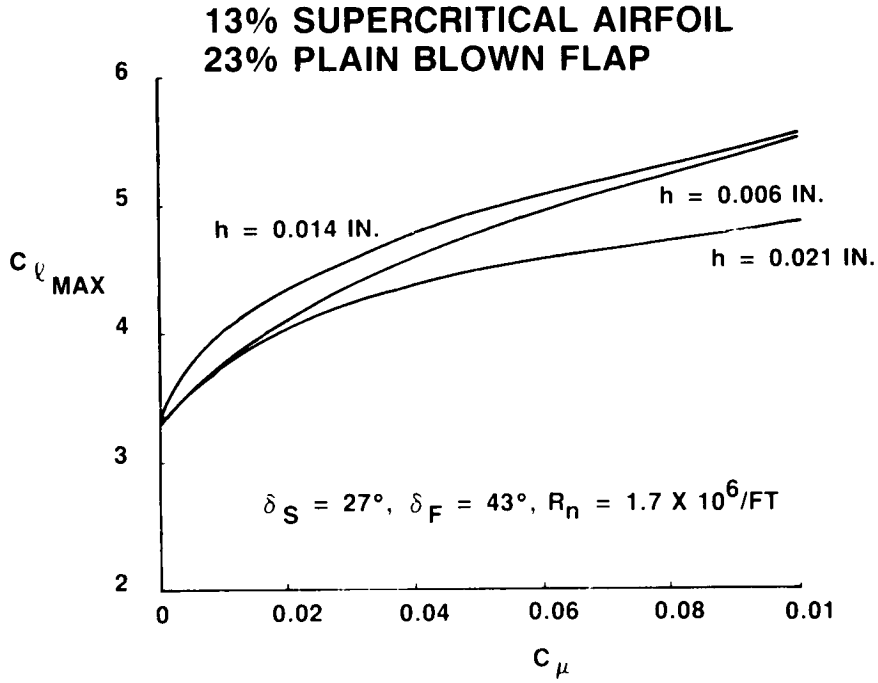

Figure 21. Effect of blowing slot height on $C_{\ell_{MAX}}$.

COMPARISON OF 2-D AND 3-D RESULTS

The plain blown flap was tested on a 1/8.5 scale model of the A-6 in the Grumman low speed wind tunnel. A comparison of the 2-D test results to the 3-D tail-off results is shown in figure 22 for equivalent test conditions. The change in clean airfoil lift is as expected due to the 3-D wing geometry. The change in C_{ℓ_α} and the change in alpha stall is evident for the clean airfoils and with blowing-on. The partial span flap area of the 3-D model results in a 60% decrease from the 2-D lift coefficient due to flap deflection plus BLC lift. The 3-D wing sweep, aspect ratio, and flap characteristics reduce the 2-D flap plus BLC lift coefficient an additional 12%. 2-D and 3-D results are not directly comparable. The lift curves in figure 22 are intended to show how 3-D effects can significantly alter the gains of a blown flap system. The effects shown can be calculated using standard 3-D prediction techniques with 2-D data.

The trimmed lift increment of the 1/8.5 scale model is shown in figure 23 as a function of C_μ. The curve shows that the 3-D test results were superior to the A-6 STOL aerodynamic design C_L's. This data, obtained at low Reynolds number conditions, verifies that the predicted STOL approach speeds of the design are attainable. The data shown indicate superior lift to the A-6/CCW demonstrator at

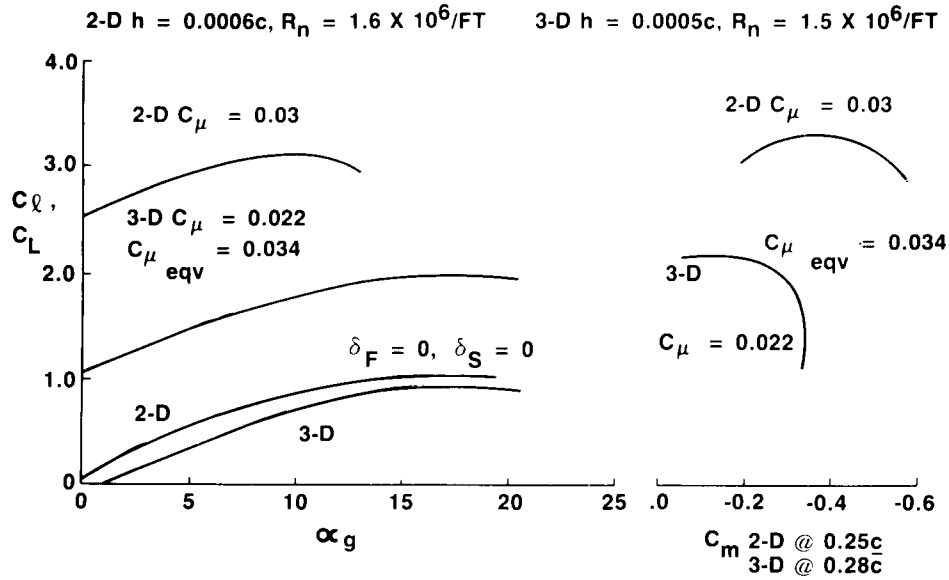

Figure 22. Comparison of 2-D to 3-D.

these low C_μ values. The A-6/CCW attained its STOL performance at C_μ's around 0.1, which is much higher than the C_μ's of the A-6 STOL. The additional lift required to obtain similar STOL performance levels is provided by deflected thrust using vectored 2-D nozzles. The combination of these two high-lift systems promises to be effective in reducing aircraft landing and takeoff speeds. The additional lifting capability can also be used to increase maximum landing weights.

CONCLUSION

The tests conducted revealed a variety of results with many interesting findings. While the data shown here indicated selection of the plain blown flap based on the available momentum, great promise was shown by the dual radius CCW. The DTNSRDC test results reported by Englar (1983) at Danvers show a fair increase in C_ℓ for a dual radius flap with a slight repositioning of the flap and increased chord. Extrapolation of that result indicates that an even larger chord dual radius may result in further increases in C_ℓ. Noting the effectiveness of the tiny chord at C_μ = 0, achieving half the lift increase of flaps with four to six times the chord length, it may be possible for a slightly larger chord dual radius CCW to outperform the plain blown flap at all C_μ levels. Some further work on the flap mechanics may lead to a reduction in the cruise and trim drag penalties of the

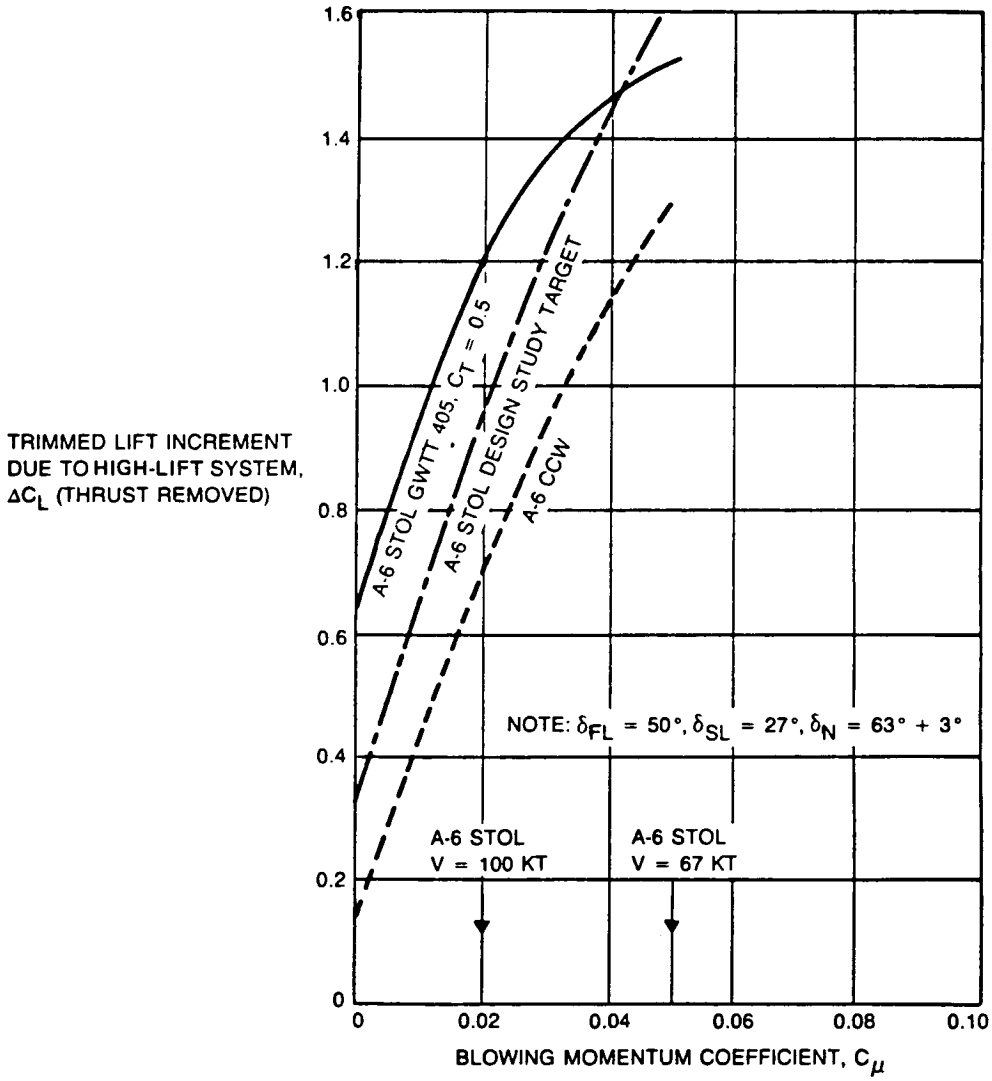

Figure 23. 3-D high-lift system ΔC_L.

trailing edge contour. Blowing over the surface during cruise to reduce C_{d_o} has been suggested; however, this is unlikely due to the high momentum required and the associated engine losses. Research should continue to define flap shape and geometry effects of blown flaps and CCW sections.

The test results also indicate that the pratical bleed levels of modern turbofan engines are the strongest driver in blown flap selection. If two or three times the blowing momentum used here were available, the merits of the dual radius and crescent blown flaps would be much stronger. Although the challenge of negating cruise and trim drag penalties would remain with higher C_μ levels to work with, the promise of these flaps would invite further investigation. The suggestion here is to study engine design to allow more bleed air to be extracted from the engine without inordinate weight penalties and/or thrust loss.

The bleed levels used in the A-6 STOL design are typical of modern turbofan engines. Doubling or tripling the available momentum is desireable to attain the full potential of lift augmentation of blown trailing edge high-lift systems on fixed wing aircraft. While additional challenges remain to be conquered, they may be addressable in an integrated design.

REFERENCES

Banks, D.W.; and Paulson, J.W., Jr.: Approach and Landing Aerodynamic Technologies for Advanced STOL Fighter Configurations. AIAA Paper No. 84-0334, AIAA 22nd Aerospace Sciences Meeting, Reno, NE, Jan. 1984.

Capone, F.J.: The Non-Axisymmetric Nozzle - It is for Real. AIAA Paper No. 79-1810, Aug. 1979.

Carr, J.E.: Aerodynamic Characteristics of a Configuration with Blown Flaps and Vectored Thrust for Low-Speed Flight. AIAA Paper No. 84-2199, AIAA 2nd Applied Aerodynamics Conference, Seattle, WA, Aug. 1984; republished as "Blended Blown Flaps and Vectored Thrust for Low-Speed Flight," AIAA J. Aircraft, vol. 23, no. 1, Jan. 1986, pp 26-31.

Cochrane, J.A.; Riddle, D.W.; and Stevens, V.C.: Quiet Research Aircraft - The First Three Years of Flight Research. AIAA Paper No. 81-2625, AIAA/NASA AMES VSTOL Conference, Palo Alto, CA, Dec. 1981.

Deckert, W.H.; and Franklin, J.A.: Powered Lift Technology on the Threshold. Aerospace America, vol. 23, no. 11, Nov. 1985, pp 34-42.

DeMeis, R.: Designing a V/STOL Fighter: McDonnell's AV-8B Harrier II. Aerospace America, vol. 23, no. 5, May 1985, pp 88-91.

Doonan, J.G.; and Callahan, C.J.: A High Speed Wind Tunnel Test Evaluation of STOL Dedicated Advanced Exhaust Nozzle Concepts. AIAA Paper No. 83-1225, AIAA/SAE/ASME 19th Joint Propulsion Conference, Seattle, WA, June 1983.

Englar, R.J.; and Husen, G.G.: Development of Advanced Circulation Control Wing High Lift Airfoils. AIAA Paper No. 83-1847, AIAA Applied Aerodynamics Conference, Danvers, MA, July 1983.

Englar, R.J.; Seredinsky, V.; et al.: Design of the Circulation Control Wing STOL Demonstrator Aircraft. AIAA Paper No. 79-1842, AIAA Aircraft Systems and Technology Meeting, New York, NY, Aug. 1979(a); republished in AIAA J. Aircraft, vol. 8, no. 1, Jan. 1981, pp 51-58.

Englar, R.J.: Subsonic Two-Dimensional Wind Tunnel Investigations of the High Lift Configuration. DTNSRDC Report ASED-79/01, Jan. 1979(b).

Englar, R.J.: Circulation Control Wing Flight Demonstrator Design Requirements and Aerodynamic Data. DTNSRDC TM-16-76-13, July 1975.

Englar, R.J.; and Williams, R.M.: Test Techniques for High Lift, Two-Dimensional Airfoils with Boundary Layer and Circulation Control For Application to Rotary Wing Aircraft. Canadian Aeronautics and Space J., vol. 19, no. 3, Mar. 1973; also presented at Annual General Meeting in Toronto, May 1972(a).

Englar, R.J.; and Ottensoser, J.: Calibration of Some Subsonic Wind Tunnel Inserts for Two-Dimensional Airfoil Experiments. DTNSRDC Report ASED AL-275, Sept. 1972(b).

Englar, Robert J.: Two-Dimensional Transonic Wind Tunnel Tests of Three 15-Percent-Thick Circulation Control Airfoils. DTNSRDC Technical Note AL-182, AD 882-075, Dec. 1970.

Holt, D.E.: C-17 Transport Employs Externally Blown Flap System. Aerospace Engineering, vol. 4, no. 1, Jan./Feb. 1984, pp 26-30.

Hudson, R.E., Jr.; and Krepski, R.E.: STOL Capability Impact on Advanced Tactical Aircraft Design. AIAA Paper No. 81-2617, AIAA/NASA Ames VSTOL Conference, Palo Alto, CA, Dec. 1981.

Lachman, G.V.: Boundary Layer and Flow Control. Vol. I and II, Pergamon Press, 1961.

Landfield, J.P.: STOL Technology for Conventional Flight Enhancement. AIAA Paper No. 84-2397, AIAA/AHS/ASEE Aircraft Design Systems and Operations Meeting, San Diego, CA, Oct. 1984.

Malavard, L.; Jousserandot, P.; and Poissen-Quinton, Ph.: Jet Induced Circulation Control; Aero Digest, Part I, Sept. 1956, pp 21-27; Part II, Oct. 1956, pp 46-59; Part III, Nov. 1956, pp 34-46.

Mashell, E.C.; and Spence, D.A.: A Theory of the Jet Flap in Three Dimensions. Proc. Royal Society, A, vol. 251, 1959, pp 407-425.

Nichols, J.H., Jr.; and Englar R.J.: Advanced Circulation Control Wing System for Navy STOL Aircraft. AIAA Paper No. 80-1825, AIAA Aircraft Systems Meeting, Anaheim, CA, Aug. 1980.

Pope, Alan; and Harper, John J.: Low-Speed Wind Tunnel Testing. John Wiley & Sons, 1966, p 186.

Pugliese, A.J.; and Englar, R.J.: Flight Testing the Circulation Control Wing STOL Demonstrator Aircraft. AIAA Paper No. 79-1791, AIAA Aircraft Systems and Technology Meeting, New York, NY, Aug. 1979.

Queen, S.; and Cochrane, J.: Quiet Short-Haul Research Aircraft Joint NAVY/NASA Sea Trials. J. Aircraft, vol. 19, no. 8, Aug. 1982, pp 655-660; presented as AIAA Paper No. 81-0152, AIAA 19th Aerospace Sciences Meeting, St. Louis, MO, Jan. 1981.

Schubauer, G.B.: Jet Propulsion with Special Reference to Thrust Augmentations. NACA TN 442, Jan. 1933.

Spence, D.A.: The Lift Coefficient of a Thin Jet-Flapped Wing. Proc. Royal Society, A, vol. 238, 1956, pp 46-68.

Williams, J.; and Butler, S.F.J.: Aerodynamic Aspects of Boundary-Layer Control for High Lift at Low Speeds. Royal Aircraft Establishment, Tech Note Aero 2858, Nov. 1962.

Yen, K.T.: An Analysis of the Flow Turning Characteristics of Upper-Surface Blowing Devices for STOL Aircraft. Report No. NADC-82007-60, Oct. 1982.